Supplement of

Two-dimensional semiconductor heterojunctions for optoelectronics and electronics

Qian Wang[1], Lin Zhang[1], Xuejuan Liu[2], and Sha Li[1*]

[1]School of Physics and Mechanical & Electrical Engineering, Hubei Engineering Technology Research Center of Environmental Purification Materials, Hubei University of Education, Wuhan 430000, China, [2]College of Physics and Engineering, Chengdu Normal University, Chengdu 611130, China

[*] E-mail: lisha@hue.edu.cn

Contents:

1. Three types of semiconductor heterojunctions

2D semiconductors have very large surface-to-volume ratio and ultrathin body thickness. Simultaneously, they also possess an atomic level of surface roughness and anisotropic physical properties (in-plane versus out-of-plane) because of strong in-plane covalent bonds and weak van der Waals interlayer interactions. Therefore, 2D semiconductors are promising heterojunction materials, and the family of 2D semiconductor heterojunctions are huge. For electronic and optoelectronic applications, 2D semiconductor heterojunctions usually have novel electronic and optical band structures, high carrier mobility, and extremely strong light–matter interactions.

Semiconductor van der Waals heterojunctions can be sorted into three types according to traditional band alignment. In type I heterojunction, both the conduction band minimum (CBM) and valance band maximum (VBM) appear in the same semiconductor, which has a narrow band gap. When type I band arrangement heterojunction is exposed to light illumination, the photo-excited electrons tend to transfer within the CBM and VBM of the narrow bandgap rather than in the broad one, spatially confine the charge carriers and efficiently reduce the undesirable dissociation of excitons, which in turn greatly improve the exciton efficiency [1]. Therefore, type-I heterojunctions are suitable for application in photoluminescence and photoluminescence excitation detection [2]. In type II heterojunctions, CBM and VBM locate at different layers, which show a staggered band alignment and thereby holes and electrons are spatially separated automatically. In addition, the vdW gap in 2D layered semiconductor heterojunction serves as weak screening of the electron−hole interaction, therefore, further extend the electron-hole recombination lifetimes [3]. Based on these features, type II band alignments are widely used for unipolar electronic, photocatalysis and photoelectric devices [4]. On the basis of type-II, the CBM in type-III heterojunction continues to reduce and eventually lower than the VBM, the band gap is broken, and the heterojunction exhibits metallic properties. The large band overlap between layers allows easier interlayer charge transfer, which accumulate the transferred holes and electrons on each side of the interface and then implement the

highly doped states [5].

2. Homojunctions and momentum-space-match in them

Homojunctions means junctions built from the same semiconductor material. Momentum match type-II junction is obtained naturally in homojunctions due to the inherent lattice orientation match between van der Waals layers of the same 2D material. Therefore, different methods are proposed to achieve homojunctions, including multiphase of the same semiconductor materials, quantum confinement effect, doping, and partial strain.

A universal approach to obtain type II band alignment in 2D semiconductor homojunctions are implemented in van der Waals multilayered semiconductors through supporting them on metal surface [6]. There are two advantages in 2D multilayered semiconductor homojunctios than 2D heterojunctions : 1) momentum-matched band alignments are easy to achieve due to the inherent lattice-orientation-match between van der Waals layers of the same 2D material; 2) largely tunable band offsets bring the conversion between band alignment types due to the charge redistribution at the junction interfaces which is controlled by the supported metal substrates.

3. Semiconductor heterojunctions composed of multiple layers

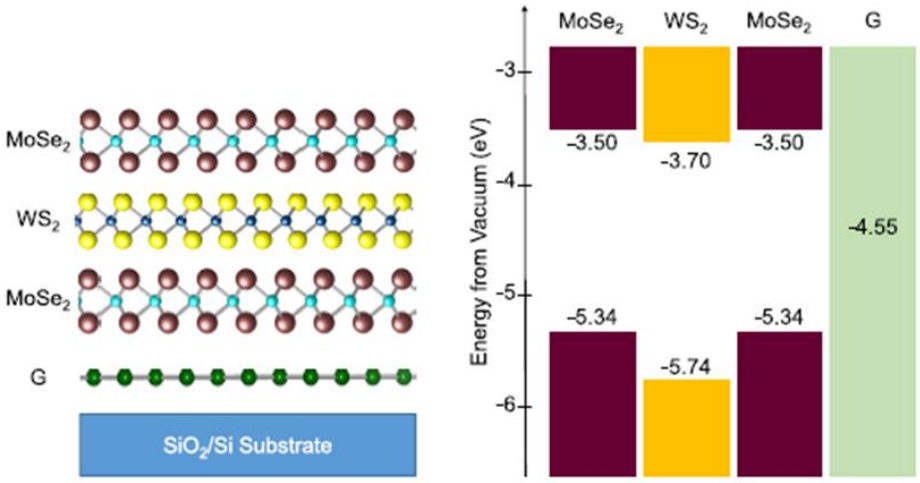

Figure. S1 Geometry structure and band alignments of the four-layer heterostructure composed of monolayers of (from substrate to top) graphene (G), $MoSe_2$, WS_2, and $MoSe_2$.

Fig. S1 displays the geometry structure and band alignment of the four-layer heterojunctions composed of monolayers graphene, $MoSe_2$, WS_2, and $MoSe_2$. Four-layer heterojunctions of $MoSe_2/WS_2/MoSe_2$/graphene were fabricated by mechanical exfoliation and dry transfer techniques. In this heterojunction, the electrons and holes are excited in both $MoSe_2$ layers, while the graphene layer is used to eliminate the carriers in the third $MoSe_2$ layer and selectively populated the first $MoSe_2$ layer with the holes which then tunnel to the third $MoSe_2$ layer. A hole tunneling time of about 20 ps is observed in the van der Waals multilayer heterojunctions, which slightly increases with the injected carrier density, and the van der Waals multilayer heterojunctions are pointing a way in sophisticated designing [7].

Besides this four-layer heterojunctions of $MoSe_2/WS_2/MoSe_2$/graphene, other multilayer van der Waals heterojunctions have also been researched, such as three-, and four-layer 2D TMDC van der Waals heterojunctions composed of 1L-MoS_2/2L-WS_2, 2L-MoS_2/2L-WS_2, and 3L-MoS_2/1L-WS_2 [8]; $MoS_2/MoSe_2/MoS_2$ heterostructure [9]; and $MoS_2/MoSe_2/MoS_2$ van der Waals heterostructure [10].

4. Janus layers heterojunction

The Janus monolayers have received increasing attention due to their broken mirror symmetry. And the Janus MoSSe monolayer has been successfully prepared [11,12]. For Janus layers heterojunctions, there are also many studies.

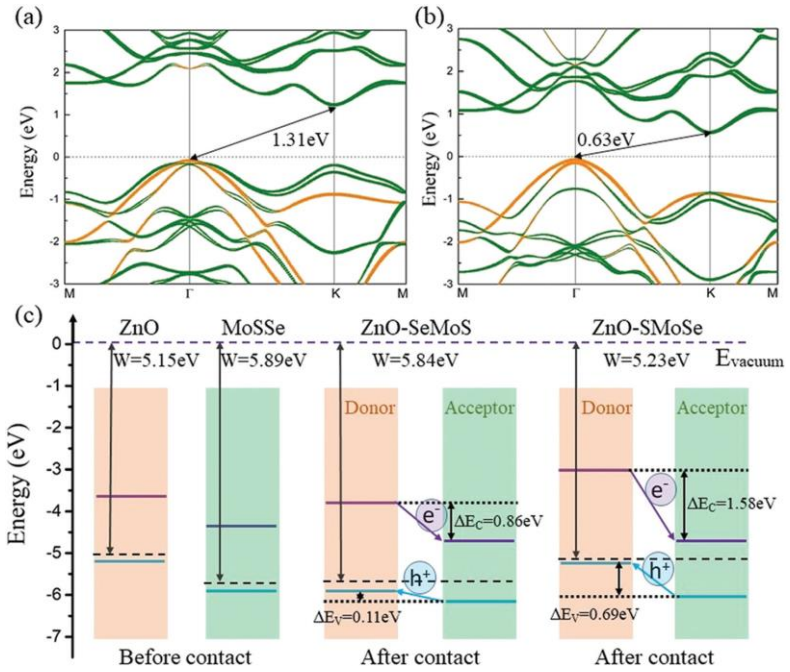

Figure S2. The projected band structures of (a) ZnO/SeMoS and (b) ZnO/SMoSe vdWHs. (c) Band alignment of the ZnO/MoSSe vdWHs [13].

The distinct character of Janus TMD is the different performance of two sides and natural built - in electric field. As shown in Fig. S2, the band gaps in ZnO/SeMoS and ZnO/SMoSe vdWHs are different, depending on the interface characteristics. In these two cases, the VBM are all located at the G point and mainly contributed by the ZnO layer, while the CBM are located at the K point and mainly consist of the MoSSe layer. The band gap of the ZnO/SMoSe heterojunction (0.63 eV) is smaller than that of ZnO/SeMoS ((1.31 eV), indicating that electrons are more easily excited from the VBM to the CBM in the ZnO/SMoSe heterostructure. Except for the band gap, the valence band offset ΔE_V and conduction band offset ΔE_C of the ZnO/SeMoS and ZnO/SMoSe heterojunctions are also different (0.11 eV and 0.86 eV for ZnO/SeMoS, and 0.69 eV and 1.58 eV for ZnO/SMoSe) due to the built-in electric field from ZnO to the MoSSe layer [13].

In addition, Li X et al. design a novel 2D Janus In_2STe/InSe vdWH and theoretically demonstrated that the vdWH is a direct-band gap (~1.23 eV) semiconductor with staggered type-II band alignment and superb optical absorption (~10^5) under ultraviolet zone [14].

5. The effect of vertical strain on the electronic behaviors of vdWHs

The effect of vertical strain on the electronic behaviors of vdWHs also deserve to research. In theoretical calculation, the vertical strain is introduced by changing the interlayer distance, since the vdW interaction plays an important role in regulating the electronic properties [15]. While in the experiment, the interlayer distance is modulated by imposing pressure with a scanning tunneling microscopy tip, inserting a dielectric layer, or vacuum thermal annealing [16,17]. Similar to biaxial strain, vertical strain can both adjust the band gap value and band alignment. The WTe_2/HfS_2 vdWH is energetically stable under vertical strain, with the type-III band alignment robustly withstand the vertical stress. The Janus-In_2STe/InSe vdWHs experience a straddling-staggered band alignment transformation with the increasing vertical strain [14].

References

[1] D. Zhang, Y. Liu, M. He, A. Zhang, S. Chen, Q. Tong, L. Huang, Z. Zhou, W. Zheng, M. Chen, K. Braun, A.J. Meixner, X. Wang, A. PanC. (2020) Room temperature near unity spin polarization in 2D Van der Waals heterostructures. Nature Communications. 11, 4442. Doi: 10.1038/s41467-020-18307-w

[2] T. Yamaoka, H.E. Lim, S. Koirala, X. Wang, K. Shinokita, M. Maruyama, S. Okada, Y. Miyauchi, K. Matsuda. (2018) Efficient Photocarrier Transfer and Effective Photoluminescence Enhancement in Type I Monolayer $MoTe_2/WSe_2$ Heterostructure. Advanced Functional Materials. 28, 1801021. Doi: https://doi.org/10.1002/adfm.201801021

[3] L. Yuan, T.-F. Chung, A. Kuc, Y. Wan, Y. Xu, Y.P. Chen, T. Heine, L. Huang. (2018) Photocarrier generation from interlayer charge-transfer transitions in WS_2-graphene heterostructures. Science Advances. 4, 2, 1700324. Doi: 10.1126/sciadv.1700324

[4] M. Palummo, M. Bernardi, J.C. Grossman. (2015) Exciton Radiative Lifetimes in Two-Dimensional Transition Metal Dichalcogenides. Nano Letters. 15, 2794-2800. Doi: 10.1021/nl503799t

[5] S. Cao, Y. Xing, J. Han, X. Luo, W. Lv, W. Lv, B. Zhang, Z. Zeng. (2018) Ultrahigh-photoresponsive UV photodetector based on a BP/ReS_2 heterostructure p-n diode. Nanoscale. 10, 16805-16811. Doi: 10.1039/c8nr05291c

[6] Q. Wang, K. Dou, X. Shi. (2020) Band alignment in multilayered semiconductor homojunctions supported on metals. Journal of Materials Chemistry C. 8, 959-967. Doi: 10.1039/C9TC04512K

[7] M. Z. Zhong,Q. L Xia, L.F. Pan,Y.Q. Liu, Y.B. Chen, H.X. Deng, J.B. Li, Z. M. Wei. (2018) Thickness-Dependent Carrier Transport Characteristics of a New 2D Elemental Semiconductor: Black Arsenic. Adv. Funct. Mater. 28, 1802581. Doi: 10.1002/adfm.201802581.

[8] M. Baranowski, A. Surrente, L. Klopotowski, J.M. Urban, N. Zhang, D.K. Maude,

K. Wiwatowski, S. Mackowski, Y.C. Kung, D. Dumcenco. (2017) Probing the Interlayer Exciton Physics in a $MoS_2/MoSe_2/MoS_2$ van der Waals Heterostructure. Nano Lett. 17, 10, 6360-6365. Doi:10.1021/acs.nanolett.7b03184.

[9] A. Surrente, Ł. Kłopotowski, N. Zhang, M. Baranowski, A. A. Mitioglu, M. V. Ballottin, P. C.M. Christianen, D. Dumcenco, Y. C. Kung, D. K. Maude, A. Kis, and P. Plochocka. (2018) Intervalley Scattering of Interlayer Excitons in a $MoS_2/MoSe_2/MoS_2$ Heterostructure in High Magnetic Field. Nano Lett. 18, 6, 3994–4000. Doi:10.1021/acs.nanolett.8b01484.

[10] H. C. Kamban., T. G. Pedersen. (2020) Interlayer excitons in van der Waals heterostructures: Binding energy, Stark shift, and field-induced dissociation. Sci Rep. 26, 10, 5537. Doi: 10.1038/s41598-020-62431-y.

[11] A. Y. Lu, H. Zhu, J. Xiao, C.P. Chuu, Y. Han, M.H. Chiu, C.C. Cheng, C.W. Yang, K.H. Wei, Y. Yang, Y. Wang, D. Sokaras, D. Nordlund, P. Yang, D.A. Muller, M.Y. Chou, X. Zhang, L.J. Li. (2017) Janus monolayers of transition metal dichalcogenides. Nat Nanotechnol. 12, 8, 744-749. Doi: 10.1038/nnano.2017.100.

[12] J. Zhang, S. Jia, I. Kholmano, L. Dong, W. B. Chen, H. Guo, Z. H. Jin, V. B. Shenoy, L. Shi, and J. Lou. (2017) Janus Monolayer Transition-Metal Dichalcogenides. ACS Nano, 11, 8, 8192–8198.

[13] P. Wang, Y. Zong, H. Liu, H. Wen, Y. Liu, H.-B. Wu, J.-B. Xia. (2021) Vertical strain and electric field tunable band alignment in type-II ZnO/MoSSe van der Waals heterostructures. Physical Chemistry Chemical Physics. 23, 1510-1519. Doi: 10.1039/d0cp05354f

[14] X. Li, B. Zhai, X. Song, Y. Yan, J. Li, C. Xia. (2020) Two-dimensional Janus-In_2STe/InSe heterostructure with direct gap and staggered band alignment. Applied Surface Science. 509, 145317. Doi: https://doi.org/10.1016/j.apsusc.2020.145317

[15] C. Lei, Y. Ma, X. Xu, T. Zhang, B. Huang, Y. Dai. (2019) Broken-Gap Type-III Band Alignment in WTe_2/HfS_2 van der Waals Heterostructure. The Journal of Physical

Chemistry C. 123, 23089-23095. Doi: 10.1021/acs.jpcc.9b07862

[16] M. Yankowitz, K. Watanabe, T. Taniguchi, P. San-Jose, B.J. LeRoy. (2016) Pressure-induced commensurate stacking of graphene on boron nitride. Nature Communications. 7, 13168. Doi: 10.1038/ncomms13168

[17] S. Tongay, W. Fan, J. Kang, J. Park, U. Koldemir, J. Suh, D.S. Narang, K. Liu, J. Ji, J. Li, R. Sinclair, J. Wu. (2014) Tuning Interlayer Coupling in Large-Area Heterostructures with CVD-Grown MoS_2 and WS_2 Monolayers. Nano Letters. 14, 3185-3190. Doi: 10.1021/nl500515q